Energy-Transfer Method to Study Vapor-Induced Latex Film Formation

Ö. PEKCAN, N. ADIYAMAN, Ş. UĞUR

Department of Physics, Istanbul Technical University, Maslak, 80626 Istanbul, Turkey

Received 10 November 2000; accepted 7 August 2001

ABSTRACT: Nonradiative energy transfer method was used to study latex film formation induced by organic solvent vapor. Seven different films with the same latex content were prepared separately from poly(methyl methacrylate) (PMMA) particles and exposed to ethyl benzene, toluene, chloroform, dichloromethane, tetrahydrofuran, and acetone vapor in seven different experiments. Energy-transfer experiments were carried out between PMMA-bound naphthalene (N) and pyrene (P) during vapor-induced film formation. Latex films were prepared from equal amounts of N- and P-labeled latex particles, and steady state spectra of N and P were monitored during film formation. It was observed that the P to N intensity ratio, I_P/I_N, increased as the vapor exposure time increased. The Prager–Tirrell (PT) model was employed to obtain back-and-forth frequencies, ν, of the reptating PMMA chains during latex film formation induced by solvent vapor. ν values were obtained and found to be correlated with the solubility parameter, δ. Polymer interdiffusion obeyed the $t^{1/2}$ law during film formation. © 2002 John Wiley & Sons, Inc. J Appl Polym Sci 84: 632–645, 2002; DOI 10.1002/app.10346

Key words: nonradiative energy transfer; latex film; vapor-induced; fluorescence; reptation frequency; crossing-density

INTRODUCTION

Latex materials are used frequently in the modern industry.[1–3] Paints, paper coatings, and water-based adhesives are commonly referred to as applications of latex. The other applications, such as pressure-sensitive adhesives, carpet backing, floor polish, condoms, gloves, textiles, coating for drug delivery, foam mattresses, composites, diapers, reinforcing fiber coating, and (potentially) bandages, are well known. Although a synthetic latex is produced in large quantities and used in many applications, many aspects of its formation still remain unknown. Many factors are known to affect the final material properties. The most difficult topic in latex film formation study is the origin of the forces that cause a latex dispersion to evolve into a continuous film. Historically, the process of film formation has been divided into three or more stages.[4–7] Definitions of the stages differ amongst authors, although the generally accepted mechanism consists of evaporation from a stable dispersion, which brings the particles into some form of close packing; deformation of particles leading to a structure without voids, although with the original particles are still distinguishable; and interdiffusion of polymer chains across particle boundaries, yielding a continuous film with mechanical integrity and with the original particles no longer being distinguishable.

Over the last several years, it has become possible to observe latex film formation at the molecular level. Small angle neutron scattering (SANS) has been used to examine deuterated particles in

Correspondence to: Ö. Pekcan (pekcan@itu.edu.tr).

Journal of Applied Polymer Science, Vol. 84, 632–645 (2002)

a protonated matrix.[8] More extensive studies have been performed using SANS by Sperling and coworkers[9,10] on compression-molded polystyrene (PS) latex films. These works covered mostly the interdiffusion process during film formation. Alternatively, the process of interparticle polymer interdiffusion has been studied by direct nonradiative energy transfer (DET), using fluorescence decay measurements in conjunction with particles labeled with appropriate donor and acceptor chromophors.[11–13] This transient fluorescence technique has been used to examine latex film formation of 1 μm in diameter, high-T_g (PMMA) particles[11] and of 100-nm in diameter low-T_g poly(butyl methacrylate) (PBMA) particles.[12,13] These studies all indicate that in the particular systems examined, annealing the films above T_g leads to polymer interdiffusion at the particle–particle junction as the particle interface heals. Atomic force microscopy (AFM) was used to observed surface topography and the packing of the PBMA system during stage II.[14] Mazur[15] has written an extensive review on the coalescence of polymer particles, in which he mainly discussed the neck growth mechanism and its several geometrical approximations before interdiffusion of polymer chains takes place. The steady state fluorescence and photon-transmission techniques have been used in our laboratory to study interdiffusion processes at the particle–particle junction during film formation and dissolution in PMMA and PS latex systems.[16–24]

In this work, various films were prepared from PMMA latex particles at stage II. Then these films were subjected to various organic vapors for latex film formation. Latex films were prepared from equal amounts of N- and P-labeled PMMA particles. Energy-transfer method and fluorescence technique were used to monitor vapor-induced latex film formation. The increase in P to N intensity ratio, I_P/I_N, with respect to solvent induction time was attributed to the increase in "crossing density" at the polymer–polymer interface. Scattered light intensity, I_{sc}, from the film surface was also monitored during film formation. Decrease in I_{sc} with increasing vapor induction time was explained by the improving quality of the latex film because of the interdiffusion of polymer chains across the junction surface.

EXPERIMENTAL

N- and P-labeled PMMA-poly isobutylene (PIB) latex particles were prepared separately by a two-step process. In the first step, MMA was polymerized to low conversion in cyclohexane in the presence of PIB containing 2% isoprene units to promote grafting. The graft copolymer produced served as a dispersant in the second stage of polymerization, in which MMA was polymerized in a cyclohexane solution of copolymer. Details have been published[24] elsewhere. A stable, spherical high-T_g dispersion of polymer particles was produced, ranging in radius from 1 to 3 μm. A combination of ^{1}H–nucelar magnetic resonance (NMR) and ultraviolet (UV) analysis indicated that these particles contain 6 mol% PIB, 0.37 mmol N, 0.037 mmol P groups per gram of polymer. We refer to these particles as N and P, respectively. (These particles were prepared in M. A. Winnik's Lab in Toronto, Canada) The molecular weight of graft PMMA were measured as 2.15×10^5 in both particles. The polydispersity of the corresponding PMMA was 1.40 for the latex particles. These particles have interpenetrating like morphologies of PIB in PMMA, with the fractal dimension of 1.89. Of the units in PMMA chains, 10% and 1% are labeled either by N or P in the corresponding particles.

Latex film preparations were carried out in the following manner: The same weights of N and P particles were dispersed in heptane in a test tube for which solid content was 0.24%. Film samples were prepared from this dispersion by placing various numbers of drops on 3×0.8-cm^2 glass plates and allowing the heptane to evaporate. Here we were careful that the liquid dispersion from the droplets covered the whole surface area of the plate and remain there until the heptane had evaporated. Samples were weighted before and after the film casting to determine the film thickness. The average film thickness was estimated to be approximately 20 μm. Average size for the particles was taken as 2 μm to estimate the number of layers or the thickness of the film samples. A LS-50 Perkin Elmer spectrophotometer (London, England) was used for fluorescence measurements.

For the film formation experiments, various solvents were chosen with different solubility parameters. Spectroscopically pure grade ethylbenzene (EB), toluene (TO), ethylacetate (EA), benzene (BE), chloroform (CH), dichloromethane (DM), tetrahydrofuran (THF), and acetone (AC) were purchased from Merck (Germany) and used as received. Characteristics of the solvent are listed in Table I.

Table I Characteristics of Solvents

Solvent	Abbreviation	$\delta(cal/cm^3)^{1/2}$	$V(cm^3/mol)$
Ethylbenzene	EB	8.8	122.5
Toluene	TO	8.9	106.3
Benzene	BE	9.1	89.1
Chloroform	CH	9.3	80.2
Dichloromethane	DC	9.7	64.0
Tetrahydrofuran	THF	9.9	81.1
Acetone	AC	10.0	73.53

Film formation experiments were performed in a 1.0 × 1.0-cm quartz cell under solvent vapor. This cell was placed in the spectrophotometer, and fluorescence emission spectra were monitored at a 90° angle. Film samples were attached to one side of the quartz cell that contains a small amount of solvent at the bottom; the film was then illuminated with 286 nm of excitation light. Peak heights of N- and P-emission spectra were monitored during the vapor-induced film formation process. The cell and the film position are presented in Figure 1. Seven different film formation experiments were run for the given solvents.

THEORETICAL CONSIDERATIONS

Energy-Transfer Method

When the incident light intensity, I_0, excites the N molecule in the film, the following mechanisms are involved:

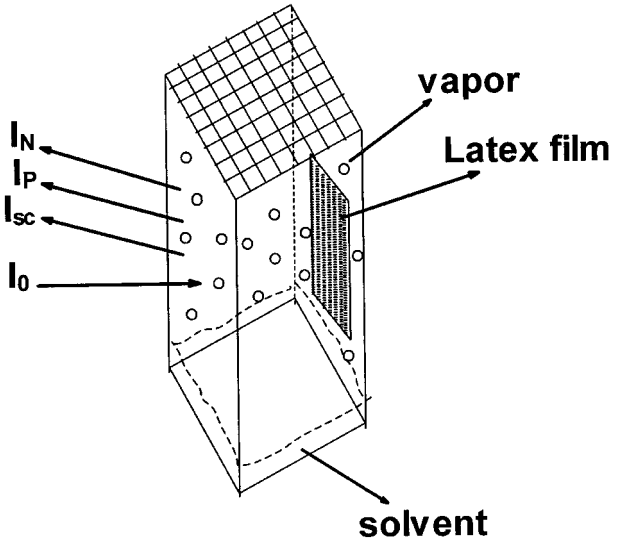

Figure 1 Fluorescence cell with latex film attached on the wall and saturated by solvent vapor. I_0, I_N, I_P, and I_{sc} are the incident (excitation), naphthalene, pyrene, and scattered light intensities, respectively.

$$N^* + P \xrightarrow{k_{ET}} N + P^*; \quad (1)$$

$$N^* \rightarrow N + h\nu_N; \quad (2)$$

$$P^* \rightarrow P + h\nu_P. \quad (3)$$

The first equation is the nonradiative energy transfer from excited naphthalene, N^*, to the P molecule with the rate constant k_{ET}. The second and third equations are the deexcitation of excited N and P to their ground states by emitting photons with the frequencies of ν_N and ν_P. The time-dependent rate equations that describe the above mechanisms for N^* and P^* can be written as

$$\frac{d[N^*]}{dt} = I_0 A_N - (k_{fN} + k_{nN})[N^*] - k_{ET}[P][N^*]; \quad (4)$$

$$\frac{d[P^*]}{dt} = I_0 A_P - (k_{fP} + k_{nP})[P^*] + k_{ET}[P][N^*] \quad (5)$$

where k_{fN} and k_{fP} are the radiative rate constants for N and P fluorescence, respectively, and k_{nN} and k_{nP} are the rate constants describing the corresponding nonradiative decay constants. A_N and A_P are the Beer's Law absorbances of N and P, respectively. The equations make explicit the fact that pyrene fluorescence has two sources: direct excitation from the incident light and energy transfer from naphthalene.

Equations (4) and (5) can be solved using the steady state hypothesis $d[N^*]/dt = d[P^*]/dt = 0$, which can provide the intensities of N (I_N) and P (I_P) emission. For convenience, we define $k_N = k_{fN} + k_{nN}$ and $k_P = k_{fP} + k_{nP}$. By definition, the

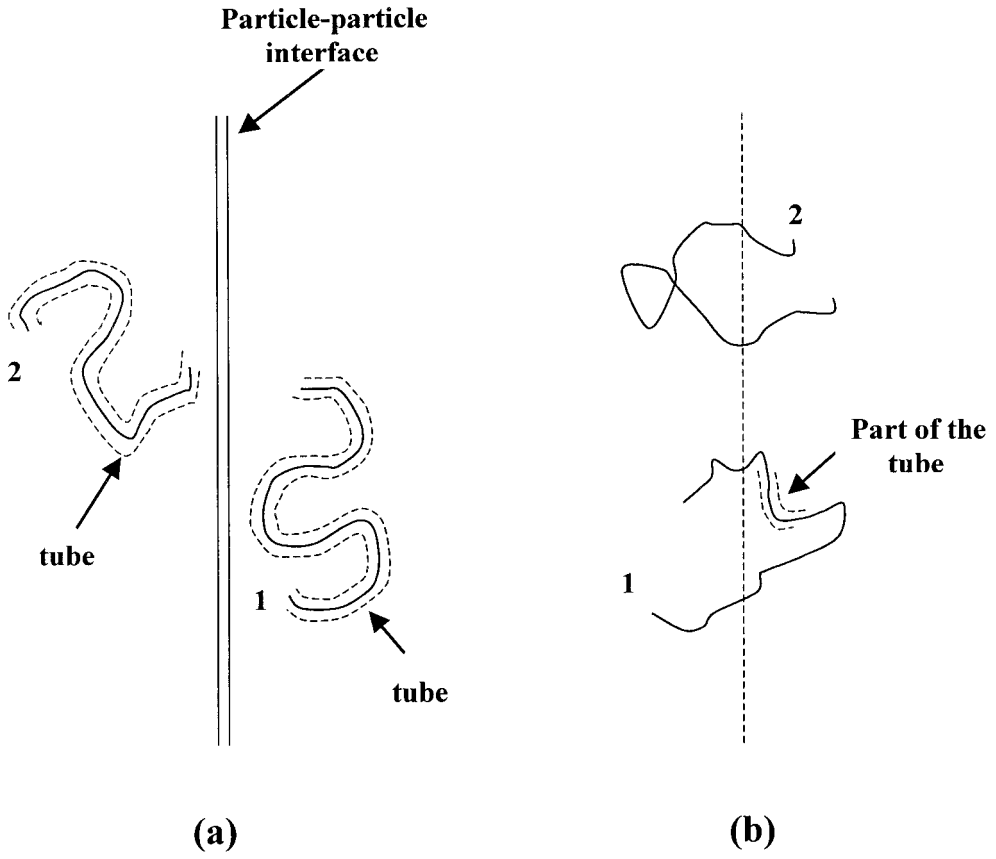

Figure 2 Cartoon representation of the reptating polymer chains in Prager–Tirrel model at (a) the polymer–polymer interface, (b) the disappeared interface. "1" represents a chain still retaining same portion in its initial tube, and "2" shows a chain relaxed at least once.

quantum yields of fluorescence from N^* and P^* are, respectively,

$$\Phi_{fN} = \frac{k_{fN}[N^*]}{I_0 A_N}; \tag{6}$$

$$\Phi_{fP} = \frac{k_{fP}[P^*]}{I_0 A_P}. \tag{7}$$

The ratio of fluorescence intensities I_P/I_N is equal to the ratio of quantum yields Φ_{fP}/Φ_{fN}, which in turn yields.

$$\frac{I_P}{I_N} = \frac{\Phi^0_{fP}}{\Phi^0_{fN}} \frac{k_P[P^*]}{\Phi^0_{fN} k_N [N^*]}, \tag{8}$$

where Φ^0_{fN} is the quantum yield of N in the absence of P, and similarly, Φ^0_{fP} is the quantum yield of P in the absence of N. Upon substitution of steady state values for $[P^*]$ and $[N^*]$, one obtains[25]

$$\frac{I_P}{I_N}\frac{\Phi_{fN}}{\Phi_{fP}} = \frac{A_P}{A_N} + \frac{k_{ET}[P]}{k_N}\left(1 + \frac{A_P}{A_N}\right). \tag{9}$$

Crossing Density

Prager and Tirrell[26] used de Gennes's "reptation" model[27] to explain configurational relaxation at the polymer–polymer junction where each polymer chain is considered to be confined to a tube in which it executes a random back-and-forth motion. Prager and Tirrell also considered a homopolymer chain with y freely jointed segments of length l that moves back and forth by one segment with frequency ν. In time, the chain displaces down the tube by a number of segments, m. Here, $\nu/2$ is called the "diffusion coefficient" of m in one-dimensional motion. Prager and Tirrell

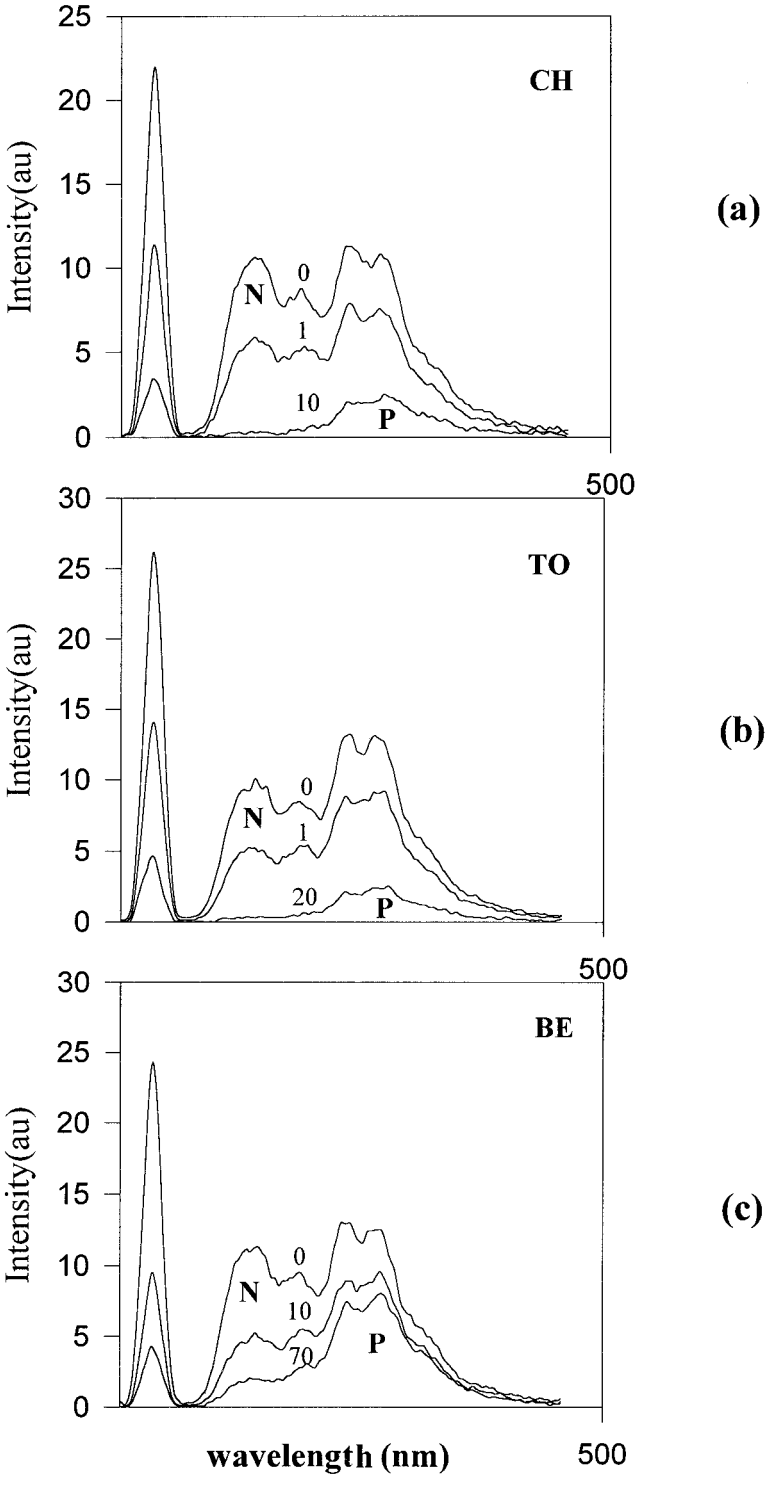

Figure 3 Fluorescence emission spectra of naphthalene (N) and pyrene (P) during organic vapor-induced latex film formation in (a) chloroform, (b) toluene, and (c) benzene. Peaks at the left-hand side of the spectra represent the scattered light intensity during film-formation processes. The number on each spectra denotes the vapor exposure time in minutes.

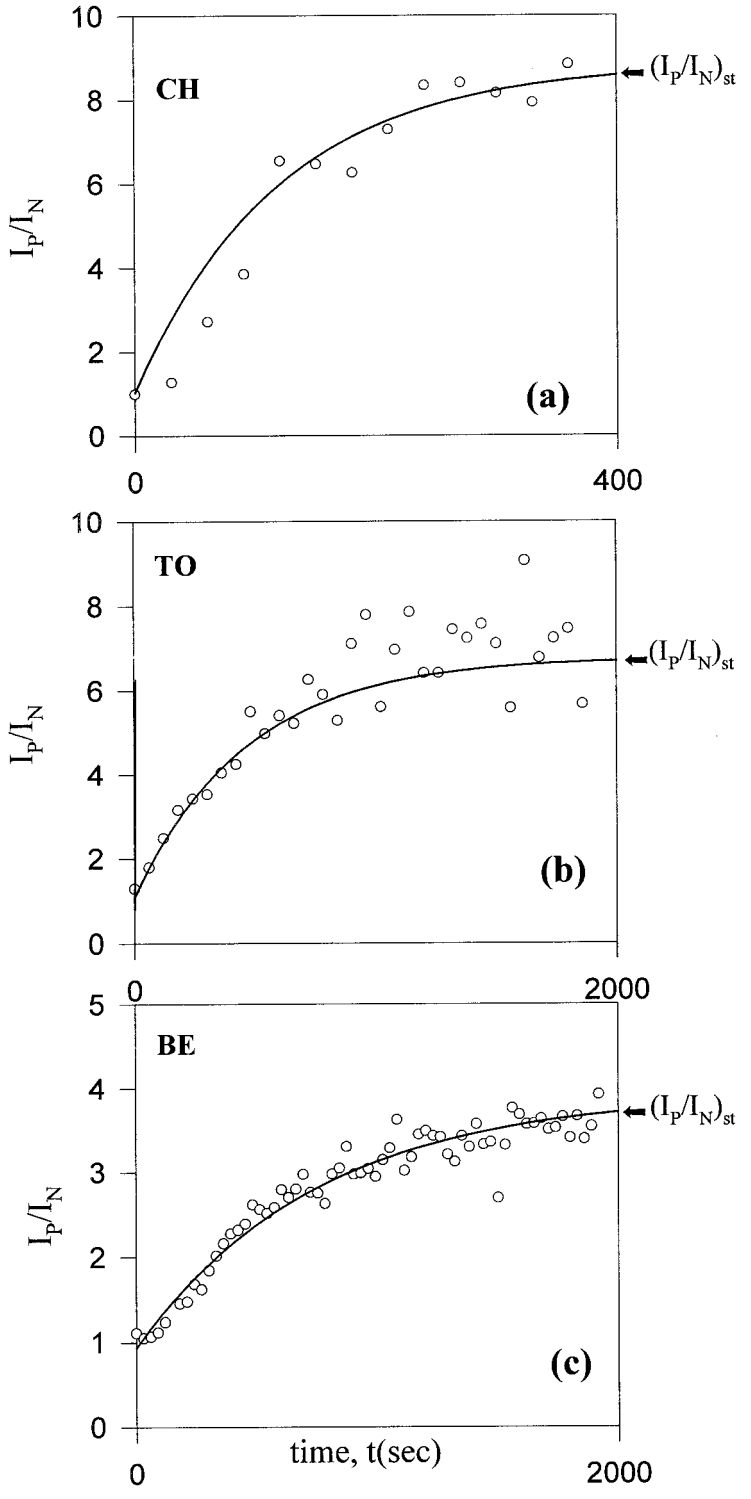

Figure 4 Plot of pyrene to naphthalene intensity ratio I_P/I_N versus vapor exposure time, t (film formation time) for (a) chloroform, (b) toluene, and (c) benzene. $(I_P/I_N)_{st}$ indicates the saturation point of (I_P/I_N).

calculated the probability of the net displacement with m during time t in the range of $m - \Delta$ to $m - (\Delta + d\Delta)$ segments. A Gaussian probability density was obtained for small times and large y. The total "crossing density" $\sigma(t)$ (chains per unit area) at the junction surface then was calculated

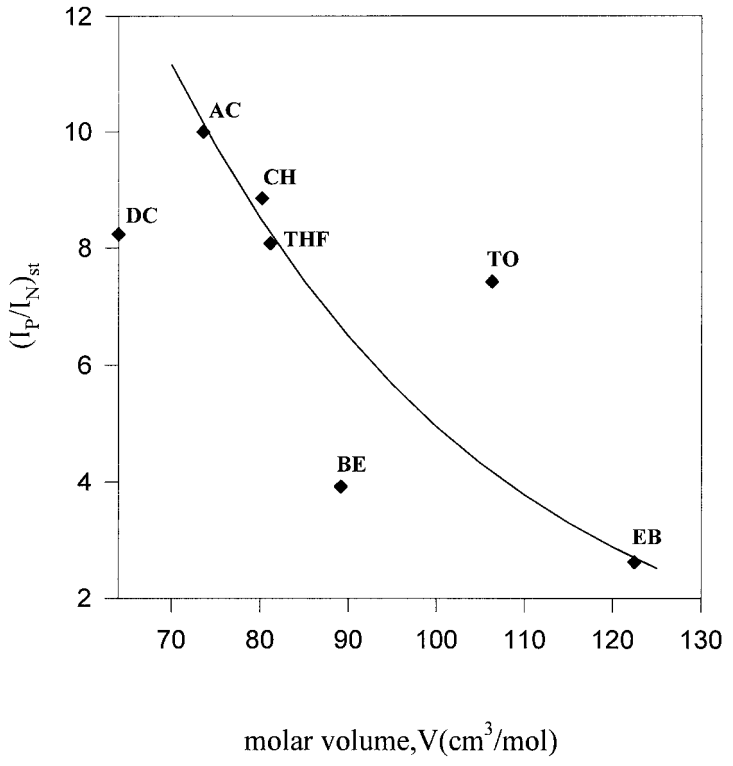

Figure 5 Plot of the plateau value, $(I_P/I_N)_{st}$ versus molar volume, V of the solvent molecules.

from the contributions caused by chains still retaining some portion of their initial tubes, $\sigma_1(t)$, plus a remainder, $\sigma_2(t)$. Here the $\sigma_2(t)$ contribution comes from chains that have relaxed at least once. σ_1 and σ_2 contributions to σ are presented in Figure 2 at the interface. In terms of reduced time $\tau = 2\nu t/y^2$, the total crossing density can be written as

$$\sigma(\tau)/\sigma(\infty) = 2\pi^{-1/2}\{\tau^{1/2} + 2\sum_{k=0}^{\infty}(-1)^n[\tau^{1/2}\exp(-k^2/\tau) - \pi^{-1/2}erfc(k/\tau^{1/2})]\}, \quad (10)$$

where n and k are the running indexes of the series. For small τ values, the summation term in the above equation is very small and can be neglected, which then results in

$$\sigma(\tau)/\sigma(\infty) = 2\pi^{-1/2}\tau^{1/2}. \quad (11)$$

This result was predicted by de Gennes on the basis of scaling arguments.

RESULTS AND DISCUSSION

Figure 3(a–c) presents the fluorescence emission spectra of N–P films when they are excited at 286 nm during the film-formation process induced by vapor of chloroform, toluene, and benzene. It is observed that P intensity, I_P, increases as N intensity, I_N, decreases, indicating that energy transfer from N to P takes place during vapor-induced film formation. In other words, P- and N-labeled PMMA chains interdiffuse during film formation, and as a result, the excited naphthalene (N^*) molecule transfers its energy to the P molecule. In the meantime, scattered light intensity, I_{sc}, at 286 nm decreases, indicating the creation of more homogeneous and transparent film.

Energy Transfer

To present the evolution of energy transfer, that is, film formation induced by vapor, I_P/I_N ratios are plotted versus time of film formation. Figure 4(a–c) presents I_P/I_N versus time plots for chloroform, toluene, and benzene, where it can be seen

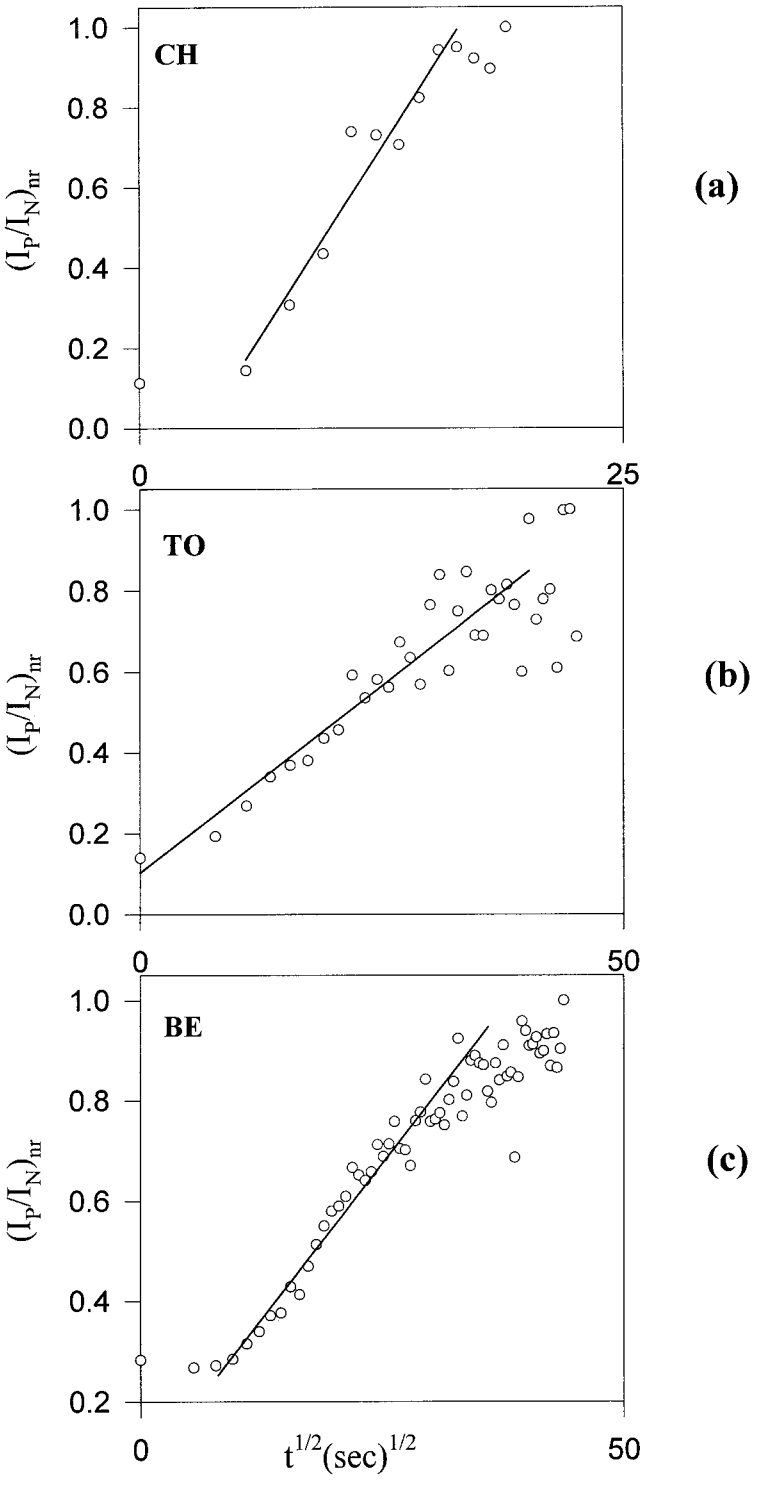

Figure 6 Plot of (I_P/I_N) according to Eq. (13) for (a) chloroform, (b) toluene, and (c) benzene. Slopes of the linear relations produce back-and-forth frequencies, ν, for the reptating polymer chains.

that all curves increase as the vapor exposure time is increased and reaches a plateau $(I_P/I_N)_{st}$ in an almost similar fashion at greater lengths of time. The chloroform sample reaches a plateau much faster than other two samples, indicating that chain interdiffusion occurs much faster in

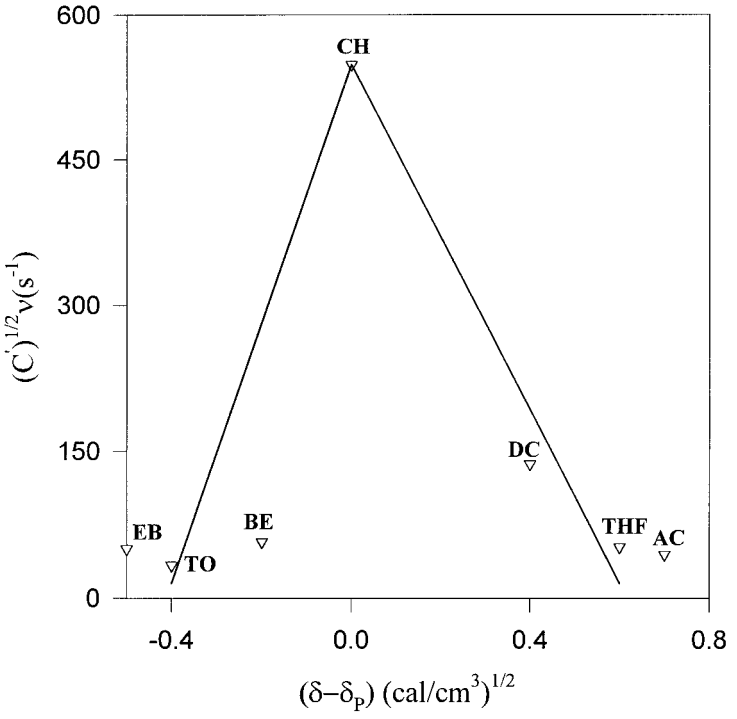

Figure 7 Plot of the relation between back-and-forth frequencies, ν, and solubility parameters, $(\delta-\delta;_P)$.

this sample than in the others. Here it is interesting to note that all I_P/I_N curves start around 1, which may indicate that there is some energy transfer between surface dyes at 0 time. At this stage, an immediate conclusion can be reached by taking into account the solvent characteristics such as molar volume, V. The plot of $(I_P/I_N)_{st}$ versus V is presented in Figure 5, where it can be seen that as the molar volume, V, increases, $(I_P/I_N)_{st}$ decreases. As $(I_P/I_N)_{st}$ is defined as the extent of energy transfer between N and P, small values of $(I_P/I_N)_{st}$ indicate the low energy-transfer values. In short, Figure 5 presents the extent of energy transfer between dye molecules at the equilibrium state of vapor uptake. Here it is observed that solvent molecule (EB) with largest V shows a lower energy transfer from N to P. However, small solvent molecules such as DC and AC present a higher amount of energy transfer from N to P at the equilibrium state of vapor-induced film formation. Here, most probably, large molecules create larger free volumes that prevent energy transfer from N to P because of longer distance between them. However, smaller free volumes created by small molecules cannot affect the energy-transfer process between N and P.

To quantify the results in Figure 4, Eq. (9) is considered by assuming that A_P absorption is negligible and can be omitted. Then Eq (9) can be written as follows:

$$\frac{I_P}{I_N} = C[P], \tag{12}$$

where

$$C = \frac{k_{ET}}{k_N}\frac{\Phi_{fP}}{\Phi_{fN}}$$

is constant for a given N–P pair. As N is excited at 286 nm, the above assumption for $A_P = 0$ is quite reasonable. Integrating Eq. (12) over the total volume, V, of latex film and assuming that the total number of P-labeled chains, P_0, crossing the interface is proportional to crossing density, $\sigma(t)$, then the following relation can be produced:

$$\frac{I_P}{I_N} = C'\nu^{1/2}t^{1/2}. \tag{13}$$

here,

$$C' = \frac{C\sigma(\infty)}{V}\left(\frac{8}{\pi N^2}\right)^{1/2}$$

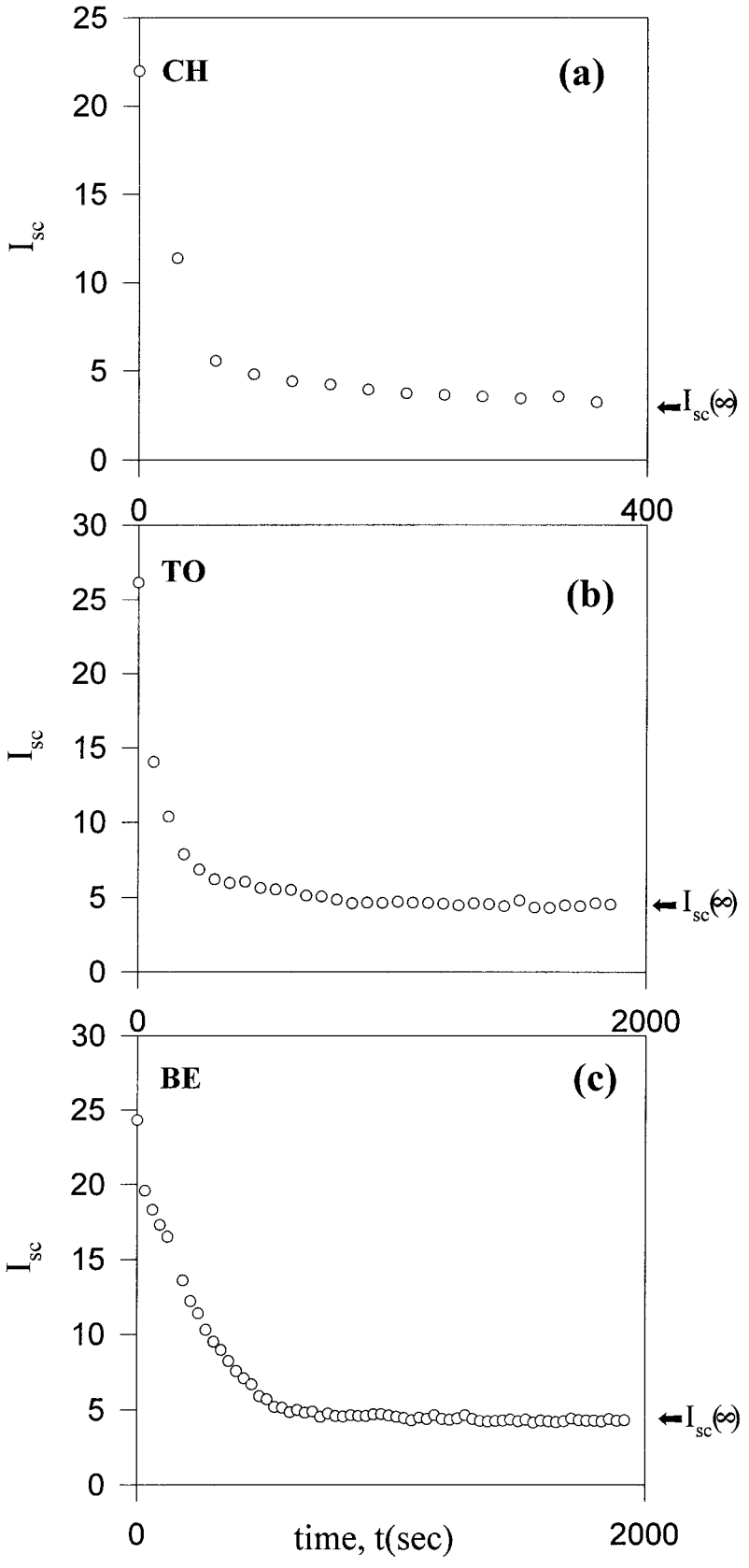

Figure 8 Plot of scattering light intensity, I_{sc} at 286 nm versus vapor exposure time, t, for (a) chloroform, (b) toluene, and (c) benzene. $I_{sc}(\infty)$ indicates the saturation point of I_{sc}.

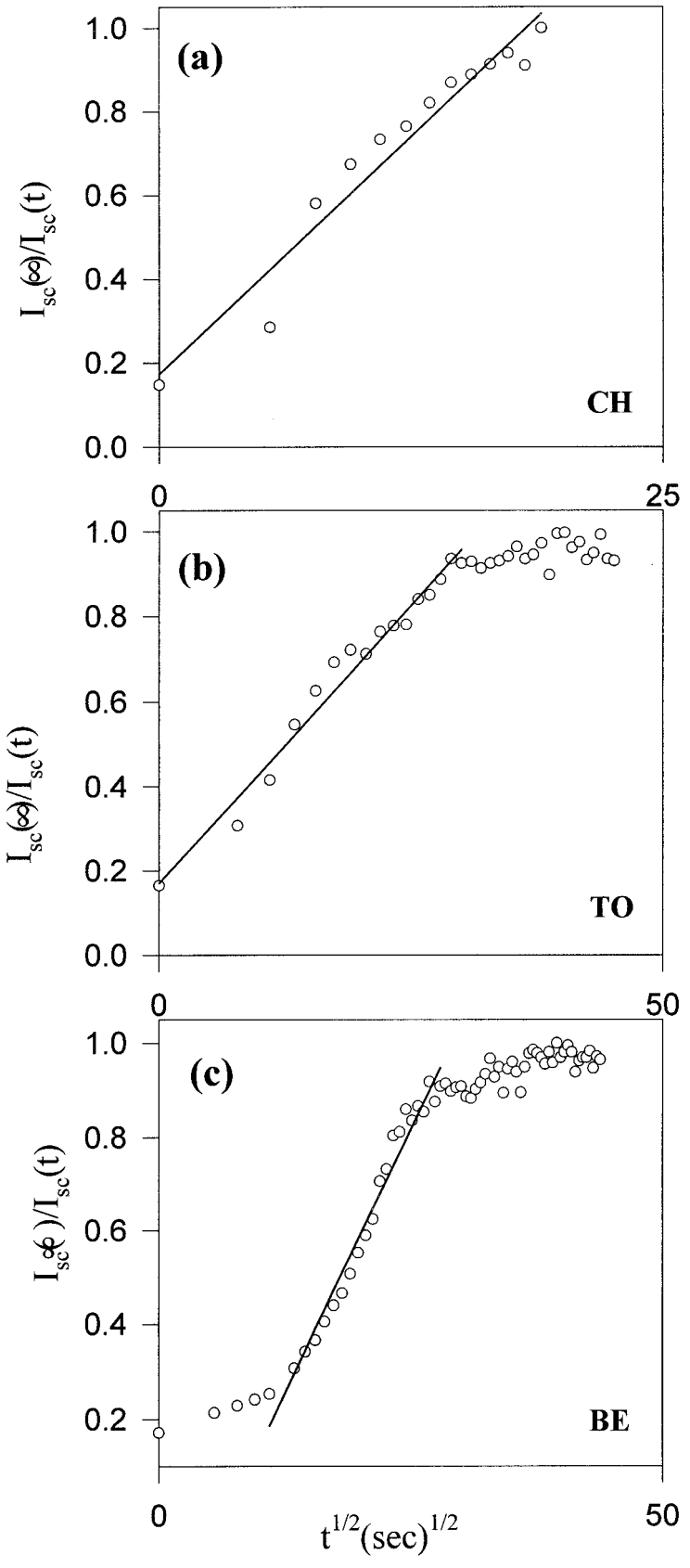

Figure 9 Plot of I_{sc} according to Eq. (13) for (a) chloroform, (b) toluene, and (c) benzene. Slopes of the linear relation produce back-and-forth frequencies, ν, for the reptating polymer chains.

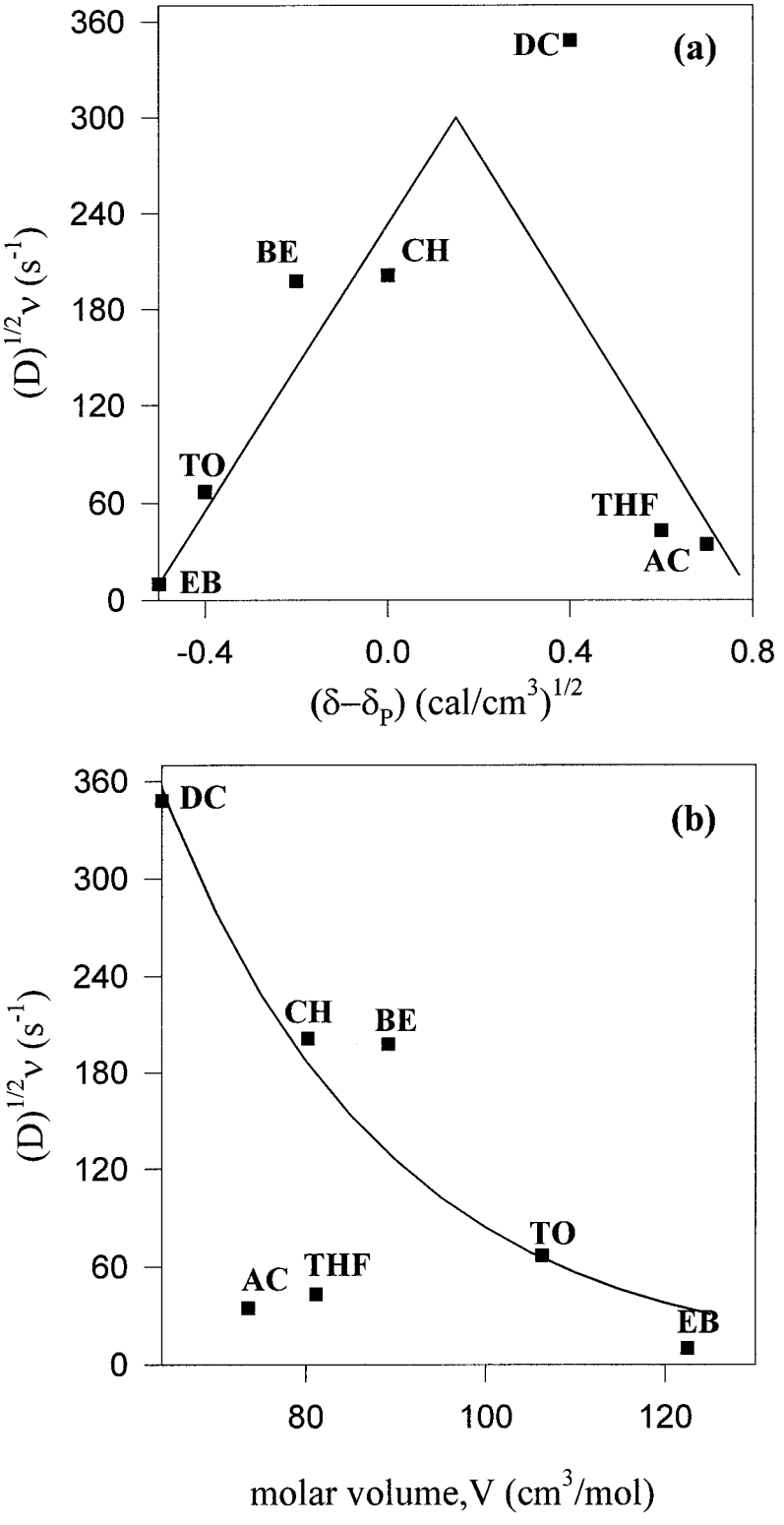

Figure 10 Plots of the relation between ν and (a) $(\delta-\delta;_P)$ and (b) V.

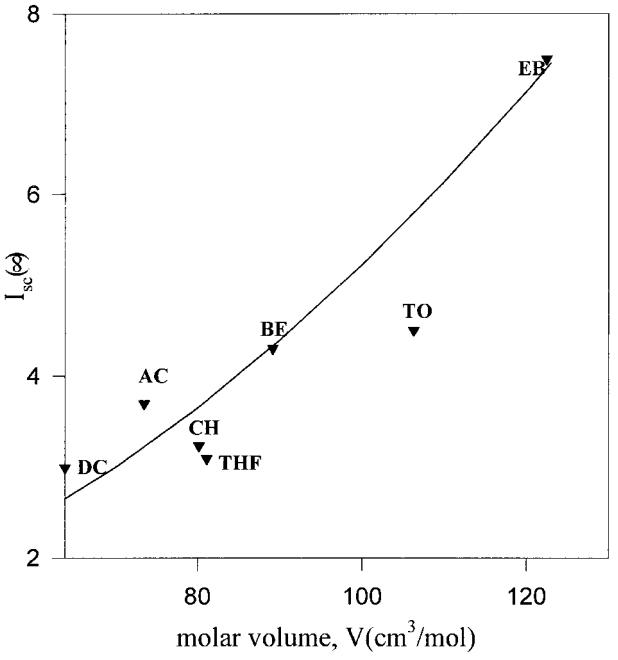

Figure 11 Plot of $I_{sc}(\infty)$ versus molar volume, V.

is taken as another constant and

$$P_0 = \int [\mathrm{P}]\, dV \tag{14}$$

was considered during integration.

The normalized $(I_P/I_N)_{nr}$ form of the data in Figure 4(a–c) are plotted in Figure 6(a–c), respectively, according to Eq. (13). Fits are nice, and support the PT model, where chain transport obeys the $t^{1/2}$ time dependence. The slope of the straight lines produce $C'\nu^{1/2}$ values, which are plotted in Figure 7. It can be seen that highest slope is produced for the CH molecule; that is, CH caused a high reptation frequency, which results in a quick interdiffusion of polymer chains. Here one immediately thinks that polymer–solvent interactions are responsible for the interdiffusion processes during solvent-induced film formation. It is well known that solution theory predicts that the polymer–solvent interaction parameter is related to the solubility parameter, δ, and the molar volume, V, via the following relation:[28]

$$\chi = \frac{V}{RT}(\delta - \delta_P)^2, \tag{15}$$

where R is the gas constant, T is the temperature, and δ_P is the solubility parameter of the polymer.

This theory leads to the conclusion that polymer material swells and that chains interdiffuse in small molecular liquid only if $(\delta–\delta_P)$ is very small. The plot in Figure 7 shows that $(\delta–\delta_P)$ approaches zero when $\sqrt{C'}v$ value is very large for the CH molecule, where $\delta_P = 9.3$ (cal/cm^3)$^{1/2}$ was taken for PMMA. From here one can conclude that the reptation frequency, ν, is strongly correlated to the polymer–solvent interaction parameter, χ, which results in quick chain interdiffusion during vapor-induced latex film formation.

Light Scattering

As seen in Figure 3(a–c), the scattered light intensity, I_{sc}, decreased as the time of vapor exposure is increased. I_{sc} versus time is plotted for CH, TO, and BE in Figure 8(a–c), respectively. These behaviors can be explained with the chain interdiffusion between latex particles during vapor-induced film formation. As the polymer chains interdiffuse, transparency of the film increases, which results in less light scattering from the latex film. These results can be related to the crossing density, $\sigma(\tau)$; that is, I_{sc} should be inversely proportional to $\sigma(\tau)$. Eq. (11) now can be written as

$$\left(\frac{I_{sc}(t)}{I_{sc}(\infty)}\right)^{-1} = D\nu^{1/2}t^{1/2}, \tag{16}$$

where $D = (8/\pi^2 y^2)^{1/2}$ is a constant. The normalized I_{sc} intensities $[I_{sc}(\infty)/I_{sc}(t)]$ are plotted in Figure 9(a–c) for the CH, TO, and BE molecules, respectively, according to Eq. (16). The slopes of the linear relations in Figure 9 produce $\sqrt{D}v$ values that are plotted in Figure 10(a and b), versus δ and V, respectively. The plot in Figure 10(a) obeys Eq. (15), which states that as the solubility parameter, δ, approaches δ_P, the polymer chain reptates faster, resulting in quick interdiffusion between latex particles. Higher value in ν for the DC molecule most probably comes from the small molar volume, V, of this solvent. The plot in Figure 10(b) indicates that small molecules penetrate deep into the latex particles, causing high-reptation frequencies for the polymer chains during vapor-induced film formation. This receives support from the $I_{sc}(\infty)$ versus V plot in Figure 11, where as V increases, $I_{sc}(\infty)$ also increases, indicating that large molecules cannot penetrate into the latex film as easily as small molecules. Films that are formed using small molecules scattered

less light than the films formed with the large solvent molecules.

In summary, this article presents a novel technique for forming latex films that can be studied using the energy-transfer method at the molecular level. This work has shown that there is strong correlation with solubility parameters and vapor-induced film formation. It has shown that polymer chains obeyed the $t^{1/2}$ law during interdiffusion to form transparent polymer films.

REFERENCES

1. Granier, V.; Sartre, A. Langmuir 1995, 11, 2179.
2. Padget, J. C. J. Coatings Tech 1994, 66, 89.
3. Müller-Mall, R. Macromol Symp 1995, 100, 159.
4. Boczar, E. M.; Dionne, B. C.; Fu, Z.; Kirk, B.; Lesko, P. M.; Koller, A. D. Macromolecules 1993, 26, 5772.
5. Wang, Y.; Winnik, M. A. J Phys Chem 1993, 97, 2507.
6. Pekcan, Ö. Trends Polym Sci 1993, 2, 236.
7. Keddie, J. L.; Meredith, P.; Jones, R. A. L;. Donald, A. M. Macromolecules 1995, 28, 2673.
8. Hahn, K.; Ley, G.; Schuller, H.; Oberthur, R. Coll. Polym Sci 1998, 66, 631.
9. Yoo, J. N.; Sperling, L. H.; Glinka, C. J.; Klein, A. Macromolecules 1990, 23, 3962.
10. Kim, K. D.; Sperling, L. H.; Klein, A. Macromolecules 1993, 26, 4624.
11. Pekcan, Ö.; Winnik, M. A.; Croucher, M. D. Macromolecules 1990, 23, 2673.
12. Zhao, C. L.; Wang, Y.; Hruska, Z.; Winnik, M. A. Macromolecules 1990, 23, 4082.
13. Wang, Y.; Zhao, C. L.; Winnik, M. A. J Chem Phys 1991, 95, 2143.
14. Juhue, D.; Lang, J. Langhuir, 1993, 9, 972.
15. Mazur, S. In Coalescence of Polymer Particles; Polymer Powder Processing; Ed. Rosenweig, N. Wiley: New York, 1995.
16. Pekcan, Ö.; Canpolat, M. J Appl Polym Sci 1996, 59, 277.
17. Canpolat, M.; Pekcan, Ö. Polymer 1995, 36, 4433.
18. Canpolat, M.; Pekcan, Ö. Polymer 1995, 36, 2025.
19. Pekcan, Ö.; Arda, E.; Kesenci, K.; Pişkin, E. J Appl Polym Sci 1998, 68, 1257.
20. Pekcan, Ö. Arda, E. J Appl Polym Sci 1998, 70, 339.
21. Arda, E. Pekcan, Ö. J Coll Interf Sci 1999, 217, 369.
22. Arda, E.; Bulmuş, V; Pişkin, E; Pekcan, Ö. J Coll Interf Sci 1999, 213, 160.
23. Pekcan, Ö.; Arda, E. Coll Surfaces A Physicochem Engin Aspects 1999, 153, 537.
24. Pekcan, Ö.; Uğur, Ş. Macromol Sym 1999, 191, 227.
25. Pekcan, Ö.; Winnik, M. A.; Egan, L. Macromolecules 1983, 16, 702.
26. Winnik, M. A. Pekcan, Ö.; Egan, L. Polymer 1984, 25, 1767.
27. Prager, S.; Tirrell, M. J. Chem Phys 1981, 75, 5194.
28. de Gennes, P. G. J Chem Phys 1971, 55, 572.
29. Flory, P. J. Principles of Polymer Chemistry; Cornell Univ. Press: Ithaca, NY, 1953.